



## Manipulating the Catalytic Property of Co-Zn Dmc for Copolymerization of Carbon Dioxide and Propylene Oxide by Modulating the Chain Length of Polyethylene Glycol

Yu Zhou<sup>1\*</sup>, Zhe Tang<sup>2</sup>, Mingyang He<sup>1</sup> and Qi Xu<sup>2</sup>

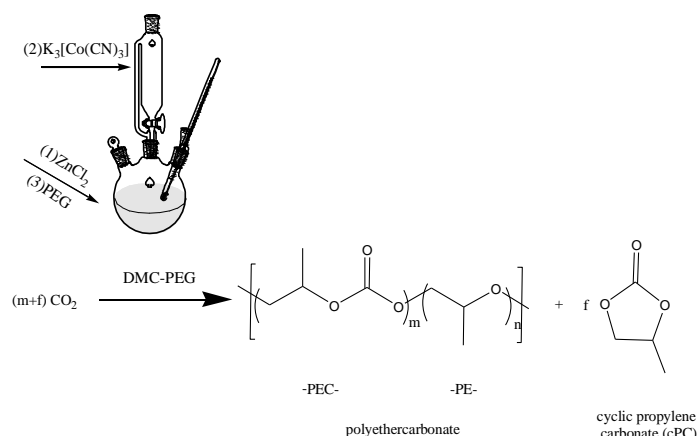
<sup>1</sup>College of Chemistry and Chemical Engineering, Changzhou University, Changzhou, Jiangsu Province, People's, Republic of China

<sup>2</sup>School of Chemistry and Chemical Engineering, Yancheng Institute of Technology, Yancheng, Jiangsu Province, People's Republic of China

### ABSTRACT

It was well known that the co-complexing agents (co-CAs) were much important for preparation of double-metal cyanide (DMC) complexes and its catalytic performance for copolymerization of CO<sub>2</sub> and propylene oxide (PO). In this work, many different Co-Zn DMCs were prepared via modulating chain length of polyethylene glycol (PEG, co-CAs), and used to catalyze copolymerization of CO<sub>2</sub> and PO. Many technologies, such as XRD, FT-IR, SEM, BET, TG, were applied to characterize these DMC catalysts. The results indicated the chain length of PEG had significantly influenced on the structure, intrinsic nature and morphology of DMC. The co-CAs PEG can stabilize the particles of DMC and induce the DMC grow preferably into the crystallinity of monoclinic phase and morphology of nano-sheets. Moreover, the co-CAs PEG can decline the interaction of C≡N and Co or Zn. All the results caused that DMC-PEG catalyst had higher CO<sub>2</sub> content, narrow PDI and moderate catalytic efficiency, compared with DMC-NONE prepared without co-CAs. In all DMC-PEG catalysts, DMC-PEG 4000 owned the best catalytic performance. Its catalytic efficiency, PDI and CO<sub>2</sub> content were 4725 g-polymer/g-Zn, 2.28 0.381, respectively.

### GRAPHICAL ABSTRACT



**Keywords:** Double metal cyanide catalyst; Co-complexing agents; Copolymerization; Carbon dioxide; Polycarbonate

## INTRODUCTION

Over the decades, one of the greatest impacts on Earth is the global warming caused by greenhouse gases such as methane, ozone, nitrous oxide and carbon dioxide (CO<sub>2</sub>). Since the industrial evolution, the concentration of CO<sub>2</sub> in the Earth's atmosphere has increased tremendously according to the latest data reported by United States National Oceanic and Atmospheric Administration on March 2014 was 399.47 ppm and increasing [1]. As known, every coin has two sides, CO<sub>2</sub> is resulted in the global warming, but also is the most fundamental carbon resource on the earth. Exploiting CO<sub>2</sub> as a participant in chemical reactions to give versatile products has received much attention since CO<sub>2</sub> has been continuously proved as an ideal synthetic feedstock in terms of abundance, cost and low toxicity [2-4]. Aliphatic polycarbonates are becoming increasingly important because of their biodegradable and semi crystalline properties similar to that of polyethylene and poly-propylene, and can be obtained through the copolymerization of CO<sub>2</sub> and epoxides with the presence of hetero-/homogeneous catalysts [5]. A wide variety of catalytic systems have been developed during the last three decades for the efficient copolymerization of CO<sub>2</sub> with epoxides, including Diethylzinc, Zinc glutarate (ZnGA), Bis(phenoxy) zinc complexes, β-diiminate (BDI) zinc complexes and double metal cyanide (DMC) catalysts [6]. One of the successful examples is the double metal cyanide (DMC) catalyst, which so far has been shown to be effective not only for ring-opening polymerization of epoxide but also for copolymerization with CO<sub>2</sub>. In particular, DMC catalysts have promising industrial prospects because of their high activity, cost-effectiveness and insensitivity to moisture. Double metal cyanides (DMCs), also known as Prussian blue analogues, are a class of molecular salts built up of a crystalline metal cyanide framework [7]. As their name suggests, DMCs feature two different metal centers, one coordinating via the carbon atom of the CN<sup>-</sup> ligand and the other via the nitrogen atom. Among various DMC catalysts, the catalyst based on Zn<sub>3</sub>[Co(CN)<sub>6</sub>]<sub>2</sub> is generally considered the best [8]. Despite the use of the same precursors, the catalytic activities of DMC catalysts were found to be profoundly dependent on the synthesis methods adopted. Pure DMC catalysts prepared in the absence of complexing agents (CAs) and co-complexing agents (co-CAs) were generally less active. Usually, organic and polymeric CAs are incorporated into the catalyst matrix to impart activity and co-CAs affect the crystallinity of catalyst. Compared to crystalline catalyst, amorphous DMC is attracting increasing interest due to enhanced catalytic performance [9,10]. In this sense, the choice of CAs and co-CAs is one of the key parameters in designing the active DMC catalysts. Currently, many reports just focus on the choice of CAs [11-16]. In fact, co-CA compounds function not only as a protecting agent to control the morphology of the catalyst but as a co-CA possibly to enhance the catalytic activity [10]. Herein, we describe the results of our study towards the preparation of DMC in the presence of PEG with the aim to control the crystallinity, composition and phase purity of catalyst. In this work, many different Co-Zn double-metal cyanide (DMC) catalysts were prepared via modulating chain length of polyethylene glycol (PEG, co-CAs), and used to catalyze copolymerization of CO<sub>2</sub> and epoxides. And it was found the chain length of PEG had significantly influenced on the structure, intrinsic nature, morphology of DMC and its catalytic performance of copolymerization of CO<sub>2</sub> and epoxides with narrow PDI. The samples were characterized by XRD, FT-IR, SEM, BET, TG and so on. In addition, many other catalysts were also investigated to compare their catalytic activity.

## EXPERIMENTAL SECTION

### Materials

Potassium hexacyanocobaltate(III) [K<sub>3</sub>Co(CN)<sub>6</sub>], Zinc chloride (ZnCl<sub>2</sub>) and tert-butyl alcohol (t-BuOH) were purchased as the analytical grade from Aladdin Reagent (Shanghai, China) without further purification. Carbon dioxide (purity more than 99.9%) were supplied from Jieyuan Air Chemical (Yancheng, China) used without further purification. Propylene oxide (PO) was refluxed over a mixture of KOH and calcium hydride (CaH<sub>2</sub>) for 48 h, then distilled and stored over 4 Å molecular sieves prior to being used in the co-polymerization reactions.

### DMC-none:

An aqueous solution of K<sub>3</sub>Co(CN)<sub>6</sub> (1.72 g of K<sub>3</sub>Co(CN)<sub>6</sub> in 20.0 mL of distilled water) was added dropwise into a ZnCl<sub>2</sub> solution (8.0 g of ZnCl<sub>2</sub> in 10.0 mL of distilled water and 10.0 mL of t-BuOH) under mechanical stirring at 50°C over a period of 1 h. White precipitation solid occurred during the addition. After completing the addition, the resulted slurry was aged at the same temperature for 2 h under stirring. The solid formed was filtered, washed with copious amount of water and dried at 60°C for 2 to 3 days to a constant weight.

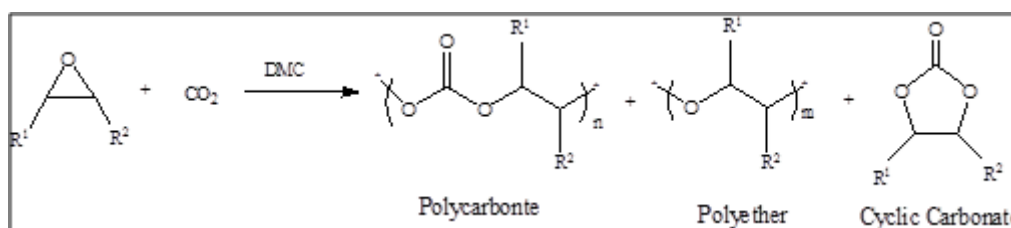
### DMC-PEG:

In the typical synthesis, solution 1 was prepared by dissolving 1.72 g of K<sub>3</sub>[Co(CN)<sub>6</sub>] in 20.0 ml of distilled water. Solution 2 was prepared by dissolving 8.0 g of ZnCl<sub>2</sub> in 10 mL of distilled water and 10.0 mL of t-BuOH. Solution 3 was prepared by dissolving 15 g of PEG-4000 in 2 mL of water and 20 mL of t-BuOH. Solution 3

was warmed to get a transparent solution. Solution 1 was added to Solution 2 at stirring over a period of 1 h. Afterwards, white solid occurred. Solution 3 was then added to above reaction mixture for another 1 h. The resulting white suspension (homogeneous colloid) was pressure-filtered and isolated. It was then re-suspended in distilled water under vigorous stirring and isolated by pressure filtration. The process was repeated at least three times. And then the sample (DMC) was obtained and dried at 60°C for 2 to 3 days to a constant weight. Other DMCs, using PEG-20000, PEG-11000, PEG-1000 and PEG-400 as co-CAs, were synthesized following the same ways with 15 g of PEG.

### Co-Polymerization of CO<sub>2</sub> and Propylene Oxide

Several co-polymerization experiments were carried out in a 100 mL stainless steel autoclave equipped with mechanical stirring and an automatic temperature control system (Scheme 1). A volume of 40 ml of PO was charged into the autoclave along with 3 mg of catalyst. The autoclave was then purged with N<sub>2</sub> three times to allow for the removal of any moisture. Finally, the autoclave was pressurized with CO<sub>2</sub> to the desired pressure and the temperature was raised and maintained at 80°C for 12 h. Upon completion of the reaction, the autoclave was cooled to room temperature and the pressure was slowly released. The resulting product was purified by dissolving in dichloromethane, then re-precipitated from methanol and dried at 50°C for further characterizations.



Scheme 1: Co-polymerization of CO<sub>2</sub> and epoxide

### Characterization

All the samples were measured by Fourier transform infrared spectra (FT-IR) testing using the KBr powder technique with diffuse reflectance sampling accessory at a resolution of 4 cm<sup>-1</sup> at room temperature on a Nicolet 460 spectrometer. The X-ray diffraction (XRD) was further used to check the crystal structures of all the samples. The powder XRD patterns of the samples were collected on a Rigaku D/MAX-2500PC diffractometer operated at 40 kV and 40mA with nickel-filtered Cu K $\alpha$  radiation ( $\lambda = 1.5406 \text{ \AA}$ ). The diffraction data was recorded in the  $2\theta$  range 2-10° with a step size of 0.02° and scan rate of 4°/min. The surface morphologies of the samples were observed by scanning electron microscopy (SEM) on a JSM-6360LV scanning electron microscope (JEOL, Japan). The thermogravimetric analyses (TGA) of the samples were carried out with a heating rate of 10°C/min under N<sub>2</sub>-atmosphere (Model: SDT Q600). The specific surface areas of the samples were determined from N<sub>2</sub> adsorption isotherms (at liquid nitrogen temperature) according to the BET method using a Quantachrome automated gas sorption system (AUTOSORB-1-C). Spectroscopic analyses of products were performed using FTIR and a Bruker NMR spectrometer (Model: Bruker AV 400 MHz) with <sup>1</sup>H, CDCl<sub>3</sub> as the solvent. Number average molecular weight (M<sub>n</sub>) and polydispersity index (PDI) of products were estimated using a gel permeation chromatography (GPC) on a Waters 515-410 system (Waters, USA) with tetrahydrofuran (THF, HPLC grade) as an eluent.

## RESULTS AND DISCUSSION

The chain length of polyethylene glycol has significant effects on crystallinity and phase purity of Co-Zn (III) DMC catalysts. DMC-NONE prepared without using co-CA PEG was highly crystalline and a typical cubic lattice structure (unit cell parameters: a=b=c=1.427nm). It showed XRD peaks at  $2\theta$  of 16.3, 19.6, 21.7, 24.6, 28.3 and 34.9° corresponding to a cubic structure with space group of Fm-3m, which can be indexed as the Prussian blue cubic space group [12-16]. However, crystal phases of the other DMC-PEG were different from DMC-NONE. After addition of PEG as co-CAs, all the crystal structures of the DMC-PEG were indexed to a mixture of cubic and monoclinic phase, and had tended from cubic phase to monoclinic phase with the increase of the chain length of PEG. And the crystallinity of the DMC-PEG was also varied with the increase of the chain length of PEG. The unit cell parameters (a) of the DMCs varied from 1.247 to 1.365 nm and the average crystallite size calculated using Debye-Scherrer equation changed from 51.1 to 64.6 nm. In general, line widths of the XRD peaks corresponding to the monoclinic phase were broader than that of the cubic phase inferring that the monoclinic crystals were smaller in size than the cubic ones [14], which implied the co-CAs PEG could prevent the DMC particles grow up. As can be seen in Figure 1, DMC-PEG4000 in all DMC catalyst had the widest diffraction, which implied the crystalline grain of DMC-PEG4000 was minimum in all DMC catalysts. The

crystalline grains of DMC catalysts increased in the order: DMC-PEG4000 < DMC-PEG400 < DMC-PEG1000 < DMC-NONE < DMC-PEG11000 < DMC-PEG120000.

### Catalyst Characterization

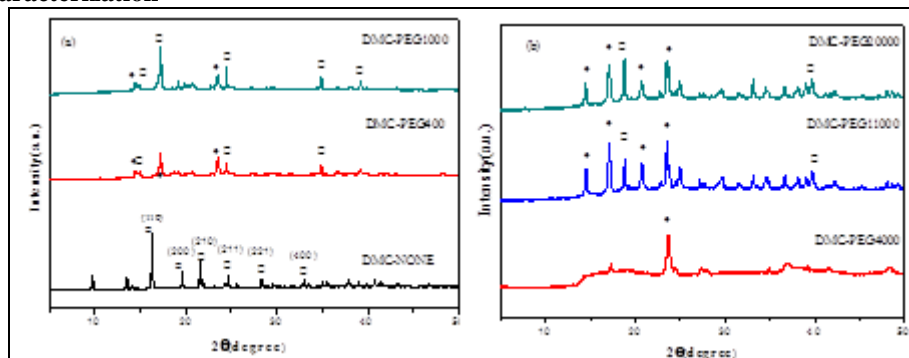


Figure 1: XRD curves of the double metal cyanide (DMC) catalysts. Peaks marked with  $\square$  correspond to cubic phase and those with  $\blacklozenge$  stand for a monoclinic phase

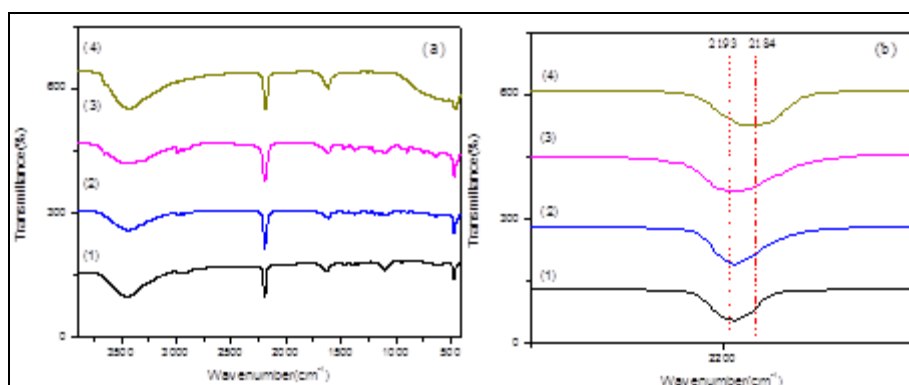


Figure 2: FT-IR spectra of DMC-PEG4000 (1), DMC-PEG1000 (2), DMC-PEG400 (3) and DMC-NONE (4)

FT-IR spectra are a powerful tool to identify the coordination and bonding of cyanide group in metal catalysts. The FT-IR data for the stretching vibrations of the  $C\equiv N$ ,  $Zn-O$  and  $Co-C$  bonds of the DMC catalysts were shown in Figure 2. From the Figure 2b, it can be seen that the  $C\equiv N$  stretching vibration band of DMC-NONE was appearing at  $2185\text{ cm}^{-1}$ , which was well agreement with the previous reports [13,16]. However, all the  $C\equiv N$  stretching vibration bands of DMC-PEG catalysts were occurring around  $2193\text{ cm}^{-1}$ . As is well known,  $C\equiv N$  act not only as  $\sigma$ -donors by donating electrons to  $Co^{3+}$  with N atom, but also as  $\pi$ - acceptor by chelating to  $Zn^{2+}$  (or zinc center catalysts) with C atom. The blue shift indicated that the mutual interaction between  $C\equiv N$  and Zn or Co became weak after addition of co-CAs PEG. Due to its well  $\sigma$ -donor and a poor  $\pi$ -acceptor of  $CN^-$ , the blue shift was mainly ascribed that mutual interaction between  $C\equiv N$  and Co with N atom become weak. Further observation of FT-IR spectra of DMC-PEG catalysts, it would be found that with the increase of chain length of co-CA PEG, the  $C\equiv N$  stretching vibration band shift and centered to  $2193\text{ cm}^{-1}$ . If the IR band at  $2184\text{ cm}^{-1}$  is ascribed to the cubic lattice structure and that at  $2193\text{ cm}^{-1}$  is belonged to monoclinic lattice structure [17,18]. The variation trend of  $C\equiv N$  stretching vibration band was well consistent with the results of XRD. Besides, there also appeared some bands at  $3445$ ,  $1382$ ,  $2976$ ,  $1099\text{ cm}^{-1}$  in DMG-PEG catalysts except DMC-NONE, which were ascribed to vibration bands of OH, C-H, C-O-C, respectively. The reason was due to the surface adsorption of a few PO. The detailed information of FT-IR of DMC catalyst can be seen in Table 1.

Figure 3 shows nitrogen adsorption - desorption isotherms and BJH pore size distribution of DMC-NONE, DMC-PEG4000, DMC-PEG400, DMC-PEG1000 and DMC-PEG11000. It can be seen that all DMC catalysts exhibited a type IV isotherm, meant there existed mesopores in all DMC catalysts. However, without co-CAs, the hysteresis loop of DMC-None was  $H_2$  type, indicated there existed ink-bottle type holes from nano-particles. While, with co-CAs, the hysteresis loops of DMC-PEG were  $H_3$  types, indicated there existed slit type holes from nano-sheet materials in the DMC-PEG. Moreover, it can be seen that as the increase of PEG chain length. The shapes of  $H_3$  types hysteresis loops DMC-PEG were becoming standard and the adsorbed quantity of  $H_3$  types hysteresis loops were increasing slowly. All the results indicated the chain length of PEG greatly affected the pore structure of DMC.

Table 1: IR wavenumber data of the double metal cyanide with different molecular weights of polyethylene glycol

Catalyst	$\nu_{C=N}(cm^{-1})$	$\nu_{C-O-C}(cm^{-1})$	$\nu_{C-O-C}(cm^{-1})$	$\nu_{CH}(cm^{-1})$	$\nu_{OH}(cm^{-1})$
DMC-PEG 4000	2194	427.3	1099	2976	3445
					1382
DMC-PEG 1000	2193	472.6	1099	2981	3438
					1373
DMC-PEG 400	2193	472.4	1105	2980	3447
					1373
DMC-NONE	2184	451.4	—	—	3422
					1378

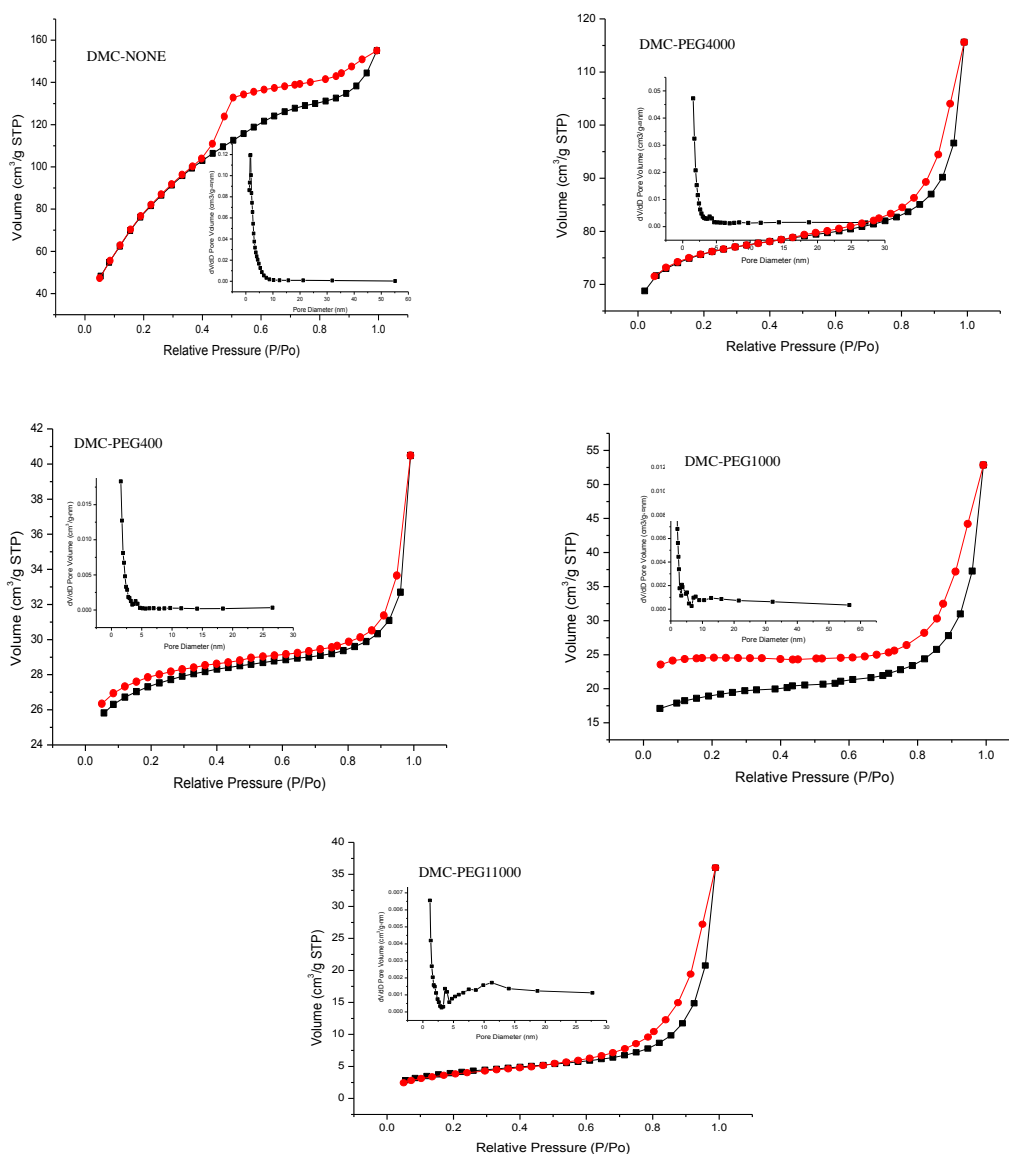


Figure 3: Nitrogen adsorption-desorption isotherms and BJH pore size distribution curves of DMC catalysts

The suppose was confirmed the results of Table 2 and SEM (Figure 4). In the Table 2, it can be seen that variation trend of specific surface area of DMCs were as following: decreased in the order: DMC-NONE(303 m<sup>2</sup>/g) > DMC-PEG4000(238 m<sup>2</sup>/g) > DMC-PEG400(84 m<sup>2</sup>/g) > DMC-PEG1000 (60 m<sup>2</sup>/g) > DMC-PEG11000(14 m<sup>2</sup>/g);

variation trend of pore volume of DMCs were in the order : DMC-NONE (0.311 ml/g) > DMC-PEG4000 (0.100 ml/g) > DMC-PEG400 (0.035 ml/g) > DMC-PEG1000(0.021 ml/g) > DMC-PEG11000 (0.001 ml/g) and average pore diameter increased in the order: DMC-NONE(1.98 nm) < DMC-PEG400(2.97 nm) < DMC-PEG4000(3.01 nm) < DMC-PEG1000 (5.46 nm) < DMC-PEG11000(15.61 nm). The BET analyses revealed that the DMC-NONE and DMC-PEG4000 had higher surface areas, which may ensure that more active sites are exposed to the reactants, thus yielding high catalytic activity.

**Table 2: The pore structure properties of DMC catalysts**

Entry	Specific surface area(m <sup>2</sup> /g)	Total pore volume(mL/g)	Average pore diameter(nm)
DMC-NONE	303.9609	0.3112	1.9835
DMC-PEG400	84.2261	0.0353	2.9737
DMC-PEG1000	59.917	0.0207	5.4565
DMC-PEG4000	238.3839	0.0995	3.0007
DMC-PEG11000	14.2853	0.0005	15.608

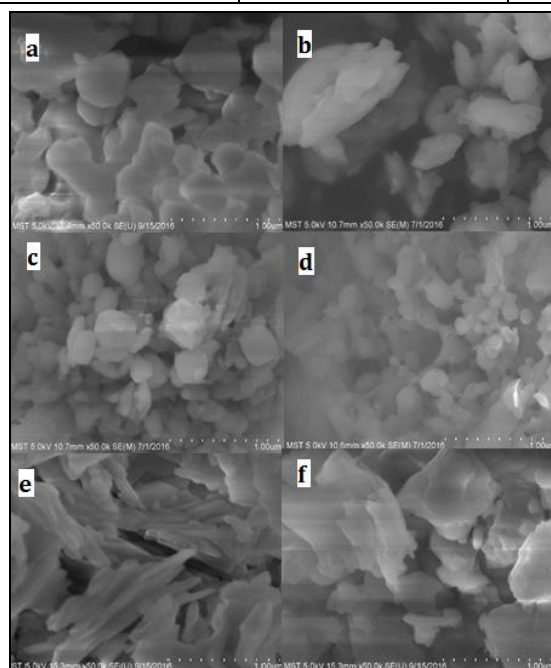


**Figure 4: SEM images of DMC-NONE(a), DMC-PEG400(b), DMC-PEG1000(c), DMC-PEG4000(d), DMC-PEG11000(e) and DMC-PEG20000(f)**

Figure 4 shows the SEM images of DMC catalysts. It can be seen as the increase of chain lengths of co-CAs PEG, the morphologies of DMC catalysts were changed gradually from amorphous nanoparticles to uniform nanosheets. DMC-NONE prepared without co-CAs PEG was the aggregations composed by a lot of irregular bulky nanoparticles (Figure 4a). When PEG400, PEG1000 and PEG4000 (Figures 4b-4d) was added, the morphologies of DMC catalyst were changed gradually from the aggregation of bulky irregular nano-particles into regular small nanoparticles. After chain lengths reach certain lengths (PEG-11000, PEG-20000), the morphologies of DMCs were changed into nanosheets and grew up gradually (Figures 4e and 4f). The results indicated the co-CAs PEG can stabilize nano-particles and induce them grow up into nano-sheet. Hence it can be concluded that the DMC-PEG 4000 had highest specific surface area and pore volume. All the results were well consistent with the results of XRD and SEM.

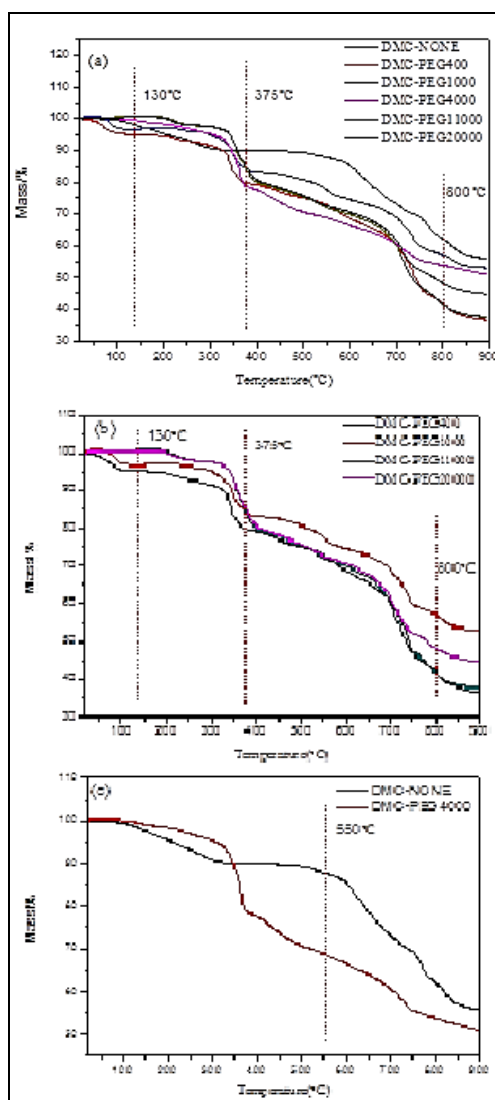


**Figure 5: Thermogravimetric analysis of Co-Zn DMC catalysts**

Thermogravimetric analyses of DMC catalysts under nitrogen atmosphere were also investigated (Figure 5). In Figure 5, three stages of weight loss were observed [19]. Stage I from 30–130°C was related to loss of water in the pores of Zn-Co DMC. These molecules of water held to the lattice through H-bonding forces and were present as solvent of crystallization. Stage II occurred in the temperature range of 130–375°C which was ascribed to loss of chemically bound water, tert-butanol (complexing agent) and PEG (co-complexing agent). Stage III from 375–800°C was attributed to decomposition of cyanide moieties. Weight loss above 800°C was due to transformation of oxides of zinc and cobalt spinel structures. (At this stage the Zn-Co cyanide salt was converted into the well-known corresponding oxides CoO and ZnO, which was Rinmann's green, and was easily recognized by the dark green color). The addition of different reagents influenced the composition (water, tert-butanol and cyanide) and crystallinity of DMC catalysts. The thermogram of DMC-NONE containing no organic co-CA showed major weight loss on the stage III, and only about 30% of weight loss was recorded at 800°C. Hence, more weight losses of the other catalysts contain co-CAs were observed (Figure 5a). Because of the varied amount of incorporated co-CAs (PEG), it was found the weight loss or decomposition of DMC catalysts below 800°C was DMC-PEG11000 (58.30%) > DMC-PEG400 (58.10%) > DMC-PEG20000 (51.70%) > DMC-PEG1000 (42.90%) (Figure 5b). It was interesting to note that DMC-PEG4000 decomposed more easily than DMC-NONE. The results indicated that grain size of DMC-PEG4000 was smaller than that of DMC-NONE, which was consistent with the results of XRD, SEM and theory described by Sebastian *et al.* [13,16].

### **Analysis of Polymer**

The cycloaddition and copolymerization of CO<sub>2</sub> and propylene oxide (PO) can occur simultaneously according to Scheme 1. The amount of the copolymer and the cycloaddition product can be counted by <sup>1</sup>H NMR as shown

in Figure 6.

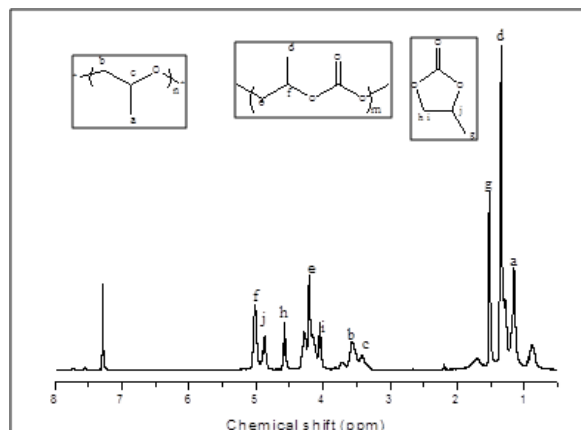


Figure 6:  $^1\text{H}$  NMR spectrum of the cyclic carbonate and poly(propylene carbonate)

Co-Zn DMCs catalyze cycloaddition and copolymerization between  $\text{CO}_2$  and PO selectively can be controlled by the reaction conditions, especially temperature. In the FT-IR spectrum (Figure 7),  $\text{C}=\text{O}$  asymmetric vibration absorption can be observed at approximate  $1743\text{ cm}^{-1}$ . Moreover, it showed a sharp  $\text{C}-\text{O}$  stretching vibration absorption at approximate  $1244\text{ cm}^{-1}$ , which provided an evidence for the presence of both carbonate and ether backbone in the resultant copolymers. In the same FT-IR spectrum, it also showed a sharp  $\text{C}=\text{O}$  asymmetric vibration absorption at approximate  $1796\text{ cm}^{-1}$  and  $\text{C}-\text{H}$  stretching vibration absorption at  $2929\text{ cm}^{-1}$ , which was assigned to the by-product (cyclic carbonate), indicating the difference from that of polycarbonate copolymer stretching vibration absorption which usually appears around  $1750\text{ cm}^{-1}$ . According to the literature [20,21], the low temperature and long reaction time may promote the growth of the polymer chain. On the other hand, promote a ring-open pathway toward the selective production of poly (propylene carbonate). Furthermore,  $^1\text{H}$  NMR spectra provide convincing evidence that product was the mixture of poly (propylene carbonate) and cyclic carbonate (Figure 8,  $^1\text{H}$  NMR: a=1.152 ppm, b=3.570 ppm, c=3.349 ppm; g=1.342 ppm; e=4.206 ppm; f=5.010 ppm; g=1.511 ppm; h= 4.000 ppm; i=4.580 ppm; j=4.903 ppm).

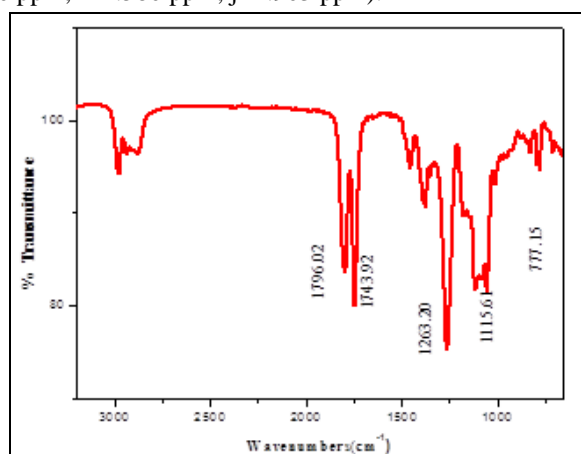


Figure 7: FT-IR spectra of cyclic carbonate and poly (propylene carbonate) prepared by DMC-PEG4000 catalyst

#### Influence of DMC Catalysts with Different Chain Lengths of Polyethylene Glycol on the Product

All co-polymerizations were performed under the same conditions ( $80^\circ\text{C}$ , 4 MPa and 12 h) by using the same amounts of catalyst and PO. As shown in Table 3, all DMCs synthesized with PEG exhibited narrow PDI (from 2.15 to 2.72), while the conventional solvent-based DMC-NONE gave broad PDI (3.79). The polymer prepared in the presence of DMC-PEG4000 had a similar carbonate linkage content (38.1%) to that of DMC-PEG1000 (32.5%) and DMC-PEG400 (35.4%), but much higher catalytic activity ( $4725\text{ g/g Zn}$ ). In order to further investigate the effect of PEG chain length on the catalytic performance, PEG-11000 and PEG-20000 were used as co-CAs. The results in Table 3 shows that DMC-PEG11000 owned low catalytic activity and DMC-PEG20000 had hardly any catalytic activity and no products was found in the DMC-PEG20000 conditions, which meant DMC-PEG4000 owned the best catalytic performance in all DMC-PEG catalysts.



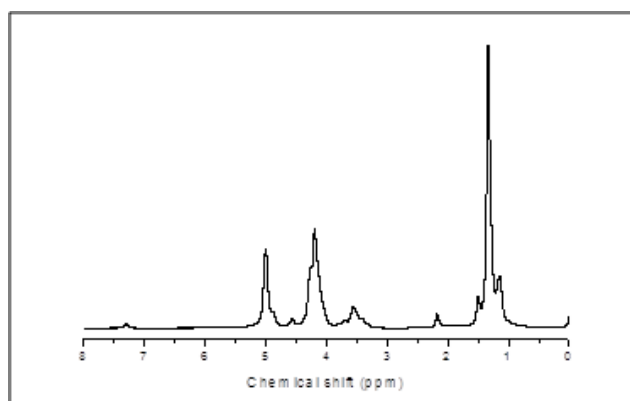


Figure 8:  $^1\text{H}$  NMR spectra of polycarbonate produced by using DMC-PEG4000 catalyst at 80, 4 MPa of  $\text{CO}_2$  for 12h

Further careful observation in Table 3, DMC-NONE prepared without co-CA PEG owned the lowest  $\text{CO}_2$  content (27.8%) and the highest catalytic activity (6596 g/g Zn) besides the widest PDI (3.79), which meant DMC-NONE was easy to catalyze PO polymerization and hard to control the reaction velocity of polymerization of PO or copolymerization of PO and  $\text{CO}_2$ . In other words, co-CA PEG can reduce the catalytic activity of DMC for polymerization of PO and improve the selectivity of copolymerization of PO and  $\text{CO}_2$ . The reason may be ascribed that PEG can induce DMC grow into monoclinic phase (from XRD results) and decline the interaction of  $\text{C}\equiv\text{N}$  and Co or Zn (from the results of FT-IR). The suppose was consistent with the conclusion by Peeters et al. [17] that was the cubic lattice structure owned more Zn vacancies in the coordination and had higher reaction activity than that of the monoclinic phase.

Table 3: Results of the copolymerization catalyzed by various DMC catalysts

Entry	Efficiency <sup>b</sup>	$\text{Fco}_2$ <sup>c</sup> (%)	$\text{Wcpc}$ <sup>c</sup> (wt%)	$\text{Mn}$ <sup>d</sup> (g/mol)	PDI
DMC-PEG20000	—	—	—	—	—
DMC-PEG11000	1134	10.7	3.41	14500	2.57
DMC-PEG4000	4725	38.1	2.73	38500	2.28
DMC-PEG1000	3112	32.5	2.17	32100	2.15
DMC-PEG400	3861	35.4	2.51	36200	2.72
DMC-NONE	6596	27.8	2.54	31500	3.79

a: Reaction condition: PO=40 ml, catalyst=3 mg,  $\text{Pco}_2$ =4 Mpa, reaction time = 12 h, reaction temperature= 80°C.

b: Efficiency of catalyst, total grams of polymer per gram of zinc.

c: The molar fraction of carbon units ( $\text{Fco}_2$ ) and the weight percentage of cyclic propylene carbonate in total product ( $\text{Wcpc}$ , wt%) were calculated by integrating the  $^1\text{H}$  NMR peak area:

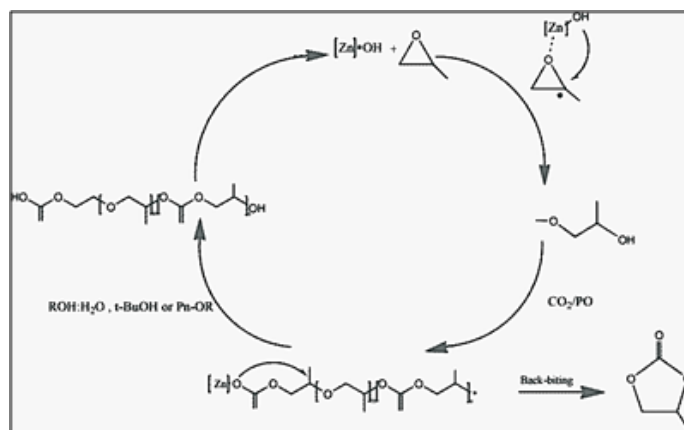
$$\text{Fco}_2 = \frac{A_{5.0} + A_{4.2} - 2A_{4.6}}{(A_{5.0} + A_{4.2} - 2A_{4.6}) + A_{3.5}} \quad \text{Wcpc} = \frac{102A_{1.5}}{102(A_{5.0} + A_{4.2} - 2A_{4.6} + A_{1.5}) + 58A_{3.5}}$$

d: Mn and PDI of the crude copolymers were determined by GPC at 35°C, using polystyrene standards for calibration.

### Possible Mechanism

The  $\text{CO}_2/\text{PO}$  copolymerization was envisaged that the polymerization reaction proceeded in two stages, the slow activation stage and the rapid propagation stage, as depicted in Scheme 2. The active site of the Co-Zn DMCs was a zinc-hydroxyl bond ( $\text{Zn-OH}$ ) based on the fact that the final product had two terminal-OH groups, as confirmed by Zhang et al. [22]. In structure, the  $\text{Zn-OH}$  bond could be functioned as a Lewis acid center, which could activate the epoxide and  $\text{CO}_2$  collaboratively during the activation stage. Meanwhile, the  $\text{Zn-OH}$  bond could trigger a further polymerization reaction and be regenerated by chain transfer, which would cause the automatic acceleration of polymerization process.

As depicted in Scheme 2, the formation of the cyclic carbonate (side product) mainly resulted from the backbiting reaction of the end carbonate anions [23]. But copolymerization reaction is not in the process of "back bite". That is, reducing backbiting reaction to inhibit the formation of cyclic carbonate.



Scheme 2: Proposed mechanism of copolymerization

Besides, Okada et al. [24] found stronger steric hindrance of epoxide suppress the backbiting reaction. Consequently, we could not only preparation of catalysts with large steric hindrances of the organic, but also use of substituent with large steric hindrances (2, 2-dimethyl, tetra-butyl, cyclohexyl, decyl, and benzy) to inhibit the formation of cyclic carbonate. At the same time, low polymerization temperature is required to avoid cyclic carbonate generation [25].

## CONCLUSION

Co-Zn DMCs were excellent catalysts for a wide range of co-polymerization reaction, particularly using epoxides. The chemical property of Co-Zn double metal cyanide catalyst prepared under different chain lengths of PEG as co-CAs was investigated. Characterizations by FT-IR, XRD, SEM, EDX and TGA were performed to confirm the morphology and structural formation of catalyst. The results were found that the co-CAs PEG can stabilize the particles of DMC and induce the DMC grow preferably into the crystallinity of monoclinic phase and morphology of nanosheets. Moreover, the co-CAs PEG can decline the interaction of C≡N and Co or Zn. All the results caused that DMC-PEG catalyst had higher CO<sub>2</sub> content, narrow PDI and moderate catalytic efficiency, compared with DMC-NONE prepared without co-CAs PEG. In all DMC-PEG catalysts, DMC-PEG 4000 owned the best catalytic performance. It's catalytic efficiency, CO<sub>2</sub> content and PDI were 4725 g-polymer/g-Zn, 2.28 0.381, respectively. At the end, we discuss possible mechanism and the possible way for inhibiting the formation of cyclic carbonate. To the best of our knowledge, this is the first report that chain length of polyethylene glycol affect the property and structure of Co-Zn DMC catalysts. This promising result is guiding us to investigate the DMC catalysts in more detail.

## Highlights

- The chain length of PEG had significantly influenced on the structure, intrinsic nature and morphology of DMC.
- PEG can decline the interaction of C≡N and Co or Zn.
- PEG can induce the DMC grow preferably from cubic phase into monoclinic phase.
- DMC-PEG catalyst owned higher CO<sub>2</sub> content, narrow PDI and moderate catalytic efficiency.
- In all DMC-PEG catalysts, DMC-PEG 4000 owned the best catalytic performance.

## ACKNOWLEDGEMENTS

Thank for the financial support from the National Key Research and Development Program of China (Grant No. 2016YFC0209203), and Jiangsu Collaborative Innovation Center for Ecological Building Materials and Environmental Protection Equipment Research Project of China. (CP201504).

## REFERENCES

- [1] CM Silva; SM Corrêa; G. Arbilla. *J Brazil Chem Soc.* **2015**, 27.
- [2] M Zaman; JH Lee. *J Korean Chem Eng.* **2013**, 30(8), 1497-1526.
- [3] J Langanke; A Wolf; J Hofmann; K Böhm; MA Subhani; TE Müller; W Leitner; C Gürtler. *Green Chem.* **2014**, 16(4), 1865-1870.
- [4] L Lei; Z Ning; W Wei; Y Sun. *Fuel.* **2013**, 108(11), 112-130.

- 
- [5] DJ Darensbourg; SJ Wilson. *Green Chem.* **2012**, 14(14), 2665-2671.
- [6] RR Ang; LT Sin; ST Bee; TT Teea; AAH Kadhumb; AR Rahmatc. *J Clean Prod.* **2015**, 102, 1-17.
- [7] C Jacek; Wojde; T Stefan; Bromley; F Illas; JC Jansen. *J Mol Model.* **2007**, 13(6-7), 751-756.
- [8] SJ Yu; Y Liu; SJ Byeon; DW Park; I Kim. *Catal Today.* **2014**, 232, 75-81.
- [9] JK Lawniczak; E Dynowska; JW Lisowski; W Sobczak; A Chruściel; W Hreczuch; J Libera; A Reszka. *X-Ray Spectrom.* **2015**, 44(5), 330-338.
- [10] IK Lee; YH Ju; C Cao; DW Parka; SH Chang; I Kim. *Catal Today.* **2009**, 148(3), 389-397.
- [11] XH Zhang; ZJ Hua; C Shang; L Fei; XK Sun; RQ Guo. *Appl Catal A.* **2007**, 325(1), 91-98.
- [12] DJ Darensbourg; MJ Adams; JC Yarbrough. *Inorg Chem.* **2002**, 40(26), 6543-6544.
- [13] J Sebastian; D Srinivas. *Appl Catal A.* **2014**, 482(5), 300-308.
- [14] A Ravindran; Anaswara; Rajendra Srivastava. *Chinese J Catal.* **2011**, 32(10), 1597-1603.
- [15] J Sebastian; S Darbha. *Rsc Adv.* **2015**, 5(24), 18196-18203.
- [16] J Sebastian; D Srinivas. *Appl Catal A.* **2013**, 464-465(6), 51-60.
- [17] A Peeters; P Valvekens; R Ameloot; ED Vos. *Acs Catal.*, **2013**, 3(4), 597-607.
- [18] PS Sreeprasanth; RSrivastava; D Srinivas; P Ratnasamy. *Appl Catal, A.* **2006**, 314(2), 148-159.
- [19] Z Radek; L Machala; MA Miroslav; V Sharma. *Crtst Growth Des.* **2004**, 4(6), 1317-1325.
- [20] J Kuyper; G Boxhoorn. *J Catal.* **1987**, 105(1), 163-174.
- [21] XB Lu; DJ Darensbourg. *Chem Soc Rev.* **2012**, 41(4), 1462-1484.
- [22] XH Zhang; RJ Wei; XK Sun. *J Polymer.* **2011**, 52(24), 5494-5502.
- [23] XH Zhang; RJ Wei; Y Zhang. *J Macromolecules.* **2015**, 48(3), 536-544.
- [24] A Okada; S Kikuchi; T Yamada. *Chem Lett.* **2011**, 40, 209-211.
- [25] S Liu; Y Qin; X Chen; X Wang; F Wang. *Polym Chem.* **2014**, 5, 6171-6179.